Proc. Natl. Acad. Sci. USA
Vol. 89, pp. 5740–5743, July 1992
Biophysics

A simple explanation of the electrostatics of the B-to-Z transition of DNA

M. GUÉRON* AND J.-P. DEMARET†

*Groupe de Biophysique, Ecole Polytechnique, 91128 Palaiseau, France; and †L.P.C.B., Institut Curie et Université Paris VI, 11 rue Pierre et Marie Curie, 75231 Paris cedex 05, France

Communicated by Alfred G. Redfield, March 9, 1992 (received for review January 2, 1992)

ABSTRACT **Whereas the phosphates of B-DNA jut out into the solution, those of Z-DNA, being closer to DNA matter, are less subject to electrostatic screening by counterions. We present simple planar models of B- and Z-DNA that reflect these geometric features. The ionic strength dependence of the difference in the Poisson–Boltzmann electrostatic free energy of the models agrees with that measured by Pohl [Pohl, F. M. (1983) *Cold Spring Harbor Symp. Quant. Biol.* 47, 113–118]. This indicates that the electrostatics of the B-to-Z transition are primarily controlled by a qualitative geometrical difference and not by details of the DNA geometry or by complex electrostatic properties of the ionic solution.**

In the B-to-Z structural transition of double-stranded DNA (e.g., sequences of alternating GC), which occurs at molar salt concentrations, the electrostatic contribution to the free energy difference, $\delta F = F_Z - F_B$, can be determined experimentally, based on the variation of the critical salt concentration with the length of the alternating GC duplex (1). This phenomenon provides an interesting test of the polyelectrolyte theories and models that are used in the study of DNA. Is the transition simple from the point of view of electrostatics, or is it a consequence of complex features of the counter-ion distribution? Does it depend on details of the polymer geometry?

In our opinion, it should be possible to explain the experimental results by using simple descriptions of both the DNA geometries and the solution electrostatics. This is because the polyelectrolyte properties are due to interactions of each charge (whether that of a DNA phosphate or that of an ion from the solution) with distant phosphates, interactions that are not sensitive to local properties.

DNA as an Impenetrable Cylinder Subject to the Poisson–Boltzmann Theory

An extensively used electrostatic model treats DNA as an impenetrable cylinder, whose radius is equal to the distance between the phosphates and the DNA axis. The charge is uniformly spread on the surface of the cylinder; the superficial charge density is such as to reproduce the linear charge density along the polyelectrolyte axis [two electronic charges per base pair; i.e., per 0.34 nm for B-DNA and per 0.37 nm for Z-DNA (2)]. The distribution of ionic charge around the cylinder is computed by the Poisson–Boltzmann theory. Contrary to the case of simply charged ions, the high linear charge of the polymer creates electrostatic potentials that are large compared to kT/e (e is the electronic charge, k is Boltzmann's constant, and T is the absolute temperature), so that the linearized (Debye–Hückel) form of the theory cannot be used.

The publication costs of this article were defrayed in part by page charge payment. This article must therefore be hereby marked "*advertisement*" in accordance with 18 U.S.C. §1734 solely to indicate this fact.

The nonlinear theory leads to two characteristic results. First, the potential at the charged surface is weakly dependent on its shape (3, 4), so that the charged plane with the same superficial charge density provides a good starting approximation, connecting the problem of polyelectrolytes to that of planar electrodes and to the field of electrochemistry. This is particularly interesting because the potential of the plane is given by a simple analytical formula (5).

Second, near the charged surface, the variation of the electric field (6), and the counterion concentration as well, are nearly independent of the salt concentration at large (4, 7). The scaling length for the variation of the electric field, which also describes the *thickness* of the ionic distribution near the surface, is designated *Th*:

$$Th = 1/(2\pi l_B z\sigma/e), \qquad [1]$$

where σ is the surface charge density, z is the counterionic valency, and l_B is the Bjerrum length, $e^2/(4\pi\varepsilon_0 DkT)$. In this expression, ε_0 and D are the absolute and relative dielectric constants, respectively. In water at room temperature, l_B = 0.72 nm. For B-DNA, represented by a charged cylinder of radius 0.95 nm (Table 1), Eq. 1 gives, in monovalent salt, *Th* = 0.226 nm.

This contrasts with the linear case, in which the scaling length is equal to λ, the concentration-dependent Debye screening length, given by

$$\lambda^{-2} = 4\pi l_B \cdot \sum n_i z_i^2, \qquad [2]$$

where n_i and z_i are the valency and concentration of ion i. In monovalent salt, λ (nm) = $(10.8\ c)^{-1/2}$, where c is the salt concentration in mol/liter.

Previous Models of the Electrostatics of the B-to-Z Transition

The first model of the B-to-Z transition used the Poisson–Boltzmann theory: each of the B and Z forms was modeled by an impenetrable cylinder of the appropriate radius and surface charge density (8). The computed slope of δF versus salt concentration is about 50 times smaller than the experimental value in the concentration range where the latter is known (1–5 M).

This failure has been ascribed to the use of the Poisson–Boltzmann theory, which, being a mean-field theory, ignores the correlations between ions in the solution. Taking into account such correlations, the variation of δF with salt concentration could be fitted to the experiment (9). In that computation, B- and Z-DNA were modeled as double-helical chains of charged beads; the models involved an adjustable parameter, the distance of closest approach between ions in the solution, to which the theoretical result was very sensitive.

Table 1. Parameters of B- and Z-DNA models

Structure	Parameter				
	Cylinder radius*	Sheath thickness†	Linear charge parameter‡	Superficial charge density§	Scaling length¶
B-DNA	0.95	0.3	4.2	1.05	0.226
Z-DNA	0.715	—‖	3.9	1.2	0.183

*Average distance of the charged phosphate oxygens to the DNA axis (computed from the data in ref. 2).

†Computed so that the volume of the sheath of the cylinder model is equal to the volume accessible to the solution between the axis of the DNA molecule (2) and the stated radius of charge.

‡This parameter, usually denoted ξ, is the charge of the polyelectrolyte per length l_B along the axis (l_B, defined in the text, is equal to 0.72 nm).

§In electron charge per nm^2 of the cylinder surface, computed as (linear charge density)/[$l_B \cdot 2\pi$(cylinder radius)].

¶In nm, given by Eq. 1.

‖The value, determined according to definition *, is 0.11 nm. However, the phosphates in Z-DNA are inequivalent. One should then distinguish two sheaths. The thickness of the inner one, corresponding to three-fourths of the charge, is about 0.05 nm. The sheaths of Z-DNA are ignored in the models computed in the text.

The Composite Cylinder Model

In this model, as in ref. 8, the electrostatics are treated in the Poisson–Boltzmann theory, and B- and Z-DNA are represented as cylinders. [Due to correlations between ions, the adequacy of the Poisson–Boltzmann approach is questionable at high salt concentrations, where the Debye length is comparable to ionic radii. However, earlier studies indicated that the problem is less serious for the properties of the counterionic distribution around polyelectrolytes than it would be for the properties of an ionic solution itself (10–13).]

We find that the experimental results can indeed be explained in this framework, provided the model incorporates the essential geometrical difference between B- and Z-DNA, from the point of view of electrostatics. This difference does not lie in the slightly smaller radius or in the slightly smaller linear charge density of Z-DNA. *It is a difference in shape*: in B-DNA, the charged phosphates jut out into the solution. They are therefore fairly well surrounded by counterions, which may be located not only beyond the phosphates but also closer to the DNA axis (i.e., in the two well-formed grooves). But in Z-DNA, the phosphates are close to the rest of the DNA matter, the major groove is shallow, and the volume of the minor groove is small, so that very few counterions can come closer to the axis than the phosphates.

For the purpose of studying the B-to-Z transition, a cylindrical model of B-DNA should therefore be a *composite*, consisting in an inner impenetrable cylinder, surrounded by a sheath filled with solution and carrying the polyelectrolyte charge on its surface. The volume of solution within the phosphate radius of B-DNA corresponds to a sheath thickness of $\approx$0.3 nm (unpublished results). In contrast, the model for Z-DNA has the charge directly on the surface of the impenetrable cylinder (Fig. 1*A*).

The above models could be refined. For instance, Z-DNA is also entitled to a sheath, albeit a much narrower one than that of B-DNA. In fact, a more precise model of Z-DNA calls for two concentric sheaths, as indicated in the legend of Table 1.

The Poisson–Boltzmann free energy for such composite cylinders has been computed. That work (unpublished results) supports our views, but the simplicity of the concept is masked to some extent by the details of the modeling and computation involved. The aim of the present work is to illustrate the composite model with an ultra-simplified case: the composite planar model. This model accounts qualitatively, to say the least, for the experimental results.

The Composite Planar Model

In the B-DNA composite cylinder model, the charged surface is surrounded by the solution both inside (the sheath) and outside, whereas in the Z-DNA model, the surface charge has the solution on the outer side only.

Furthermore, the surface potential of a highly charged cylinder is close to that of a plane with the same surface charge density (4) (except at very low salt concentrations, a case not considered here).

Therefore the free-energy difference may be approximated as that between two charged planes, a B "two-faced plane" with solution on both sides (extending to infinity on one side and up to a distance equal to the sheath thickness on the other) and a Z "one-faced plane" with solution on one side.

To compute the free energy of this model, a useful intermediate is the counterionic charge in the sheath. Unfortunately, its evaluation is a bit complicated because it depends on the ionic strength and on the superficial charge density, which varies during the charging process used for computing the free energy.

We therefore introduce a last simplification, which has the disadvantage of modifying the counterionic charge in the sheath, but the advantage that the free energy of the resulting model is obtained extremely easily. The simplification consists in letting the thickness of the sheath become infinite. Because the sheath thickness of B-DNA is larger than the scaling length *Th* for the fully charged cylinder (Table 1), we estimate that the resulting increase of the counterionic charge is not large enough to make the model severely misleading. Rather, we consider that the extension of the B-DNA sheath is in the same spirit as the reduction of the sheath of Z-DNA to zero; each of these simplifications enhances, spuriously but not severely, the difference between the B-DNA and Z-DNA models.

Let ϕ be the reduced potential (the potential divided by e/kT). In a salt of z-valent counterions and $-z$-valent coions, its value at the surface of the one-faced plane with surface charge density σ (5) is

$$\phi_{\text{surface}}(\sigma, \lambda) = (2/z)\sinh^{-1}(\lambda/Th). \quad [3]$$

This expression is exact in the linear and nonlinear range. The free energy per electronic charge (phosphate) is obtained by the usual charging process:

$$F(\sigma, \lambda) = kT \int_0^1 \phi_{\text{surface}}(s\sigma, \lambda)ds. \quad [4]$$

Hence,

$$F(\sigma, \lambda)/(2kT/z) = \sinh^{-1}(1/x) + x - (1 + x^2)^{0.5}, \quad [5]$$

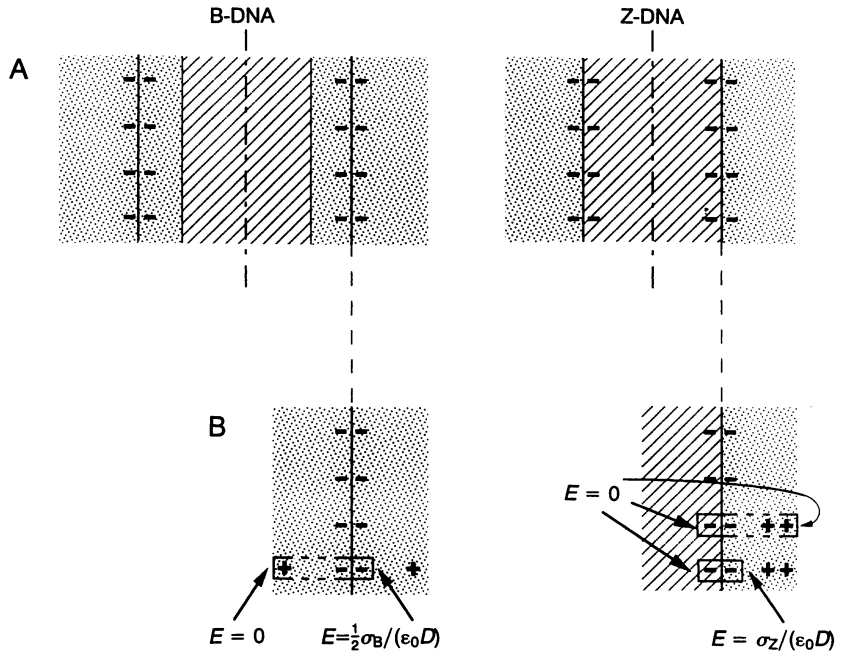

FIG. 1. (*A*) Cylindrical models for B-DNA, an impenetrable cylinder within a solution-filled sheath, and for Z-DNA, an impenetrable cylinder. The superficial charge density σ is, as usual, the one that gives the correct linear charge density [e.g., 2 electronic charges per 0.34 nm for B-DNA and per 0.37 nm for Z-DNA (Table 1)]. (*B*) Planar models for B-DNA, a plane layer of charge immersed in the solution, and for Z-DNA, a plane layer with the solution on one side. The electric field at the surface was determined by application of Gauss's theorem to three different volumes, two of which include neutralizing counterions as shown. The polyelectrolyte charge is split in two for this purpose, as pictured by the dual "−" signs. The values of the electric field are indicated. The symbol ε_0 stands for the absolute dielectric constant, and D is the relative dielectric constant of water.

with

$$x = Th/\lambda. \qquad [6]$$

We now establish the relation between the free energy of a one-faced plane, $F_{one}(\sigma)$ (given by Eq. 5), and that, $F_{two}(\sigma)$, of the two-faced plane with the same surface charge density σ. In the former case, all the neutralizing ions are on one side. In the second case, the ions on each side neutralize half of the surface charge. (The argument is best followed by considering Fig. 1*B* and temporarily ignoring the different subscripts to σ.) Applying Gauss's theorem for the flux of the electric field to a box enclosing a section of the plane surface and extending to infinity, one sees that a two-faced plane with surface charge density σ creates the *same* electric field at the interface with the solution as a one-faced plane with surface charge density $\sigma/2$. This condition, together with that of zero field and potential at infinity, leads to identical surface potentials. Hence, the free energy, obtained by the charging procedure, is also the same:

$$F_{two}(\sigma) = F_{one}(\sigma/2). \qquad [7]$$

The free energy difference is, therefore,

$$F_Z - F_B \equiv F_{one}(\sigma_Z) - F_{two}(\sigma_B) = F_{one}(\sigma_Z) - F_{one}(\sigma_B/2), \qquad [8]$$

where F_{one} is given by Eq. 5 with the appropriate values of σ and of x (Eqs. 1 and 6).

The results, which require no computation beyond the evaluation of Eq. 5, are plotted in Fig. 2*B*. The computation was done for two models of DNA. For the solid line, the radius is the average distance from the axis to the charged oxygens of the phosphate groups—namely, 0.95 nm for B-DNA and 0.715 nm for Z-DNA (Table 1). The dashed line was computed with the radii from the earlier Poisson–Boltzmann study (8), 1 and 0.9 nm, and with the corresponding charge densities, 0.928 and 1.03 electronic charge per nm^2. The salt is monovalent.

The dotted line is the result derived from the experimental measurements in sodium chloride solutions. Since it includes an unknown, constant, nonelectrostatic component, only its variation with the salt concentration is significant for comparison with the theory. The slope of the solid line is practically equal to the experimental one. That of the dashed line is 75% of the latter, as compared to only 2% in the earlier model using the same DNA radii.

Considering the approximations made, as well as the limited amount of experimental results (no detailed measurements have been reported for other ions than NaCl), the excellent agreement between the theoretical (solid line) and experimental slopes is satisfying, but it must be partly fortuitous. The important points are that (*i*) the slope has the right sign and order of magnitude and (*ii*) agreement with the experiment is robust with respect to changes in the radii of the charged cylinders representing DNA.

Conclusion

In conclusion, it appears that the electrostatic contribution to the enhanced stability of B-DNA over Z-DNA in lower salt is due essentially, and at least semiquantitatively, to the simple fact that, in the B geometry, the phosphate charges are well immersed in the solution and thus may be better surrounded with counterions, and better screened by them, than in the Z geometry. This property can be accounted for by a composite cylindrical model treated in the Poisson–Boltzmann theory.

We shall present elsewhere a computation of the free energy difference in composite cylindrical models of DNA, based on analytical formulae and approximations for the Poisson–Boltzmann potential (4, 6). It may be interesting to compare the results thus obtained with those of a numerical Poisson–Boltzmann computation of the composite cylinder

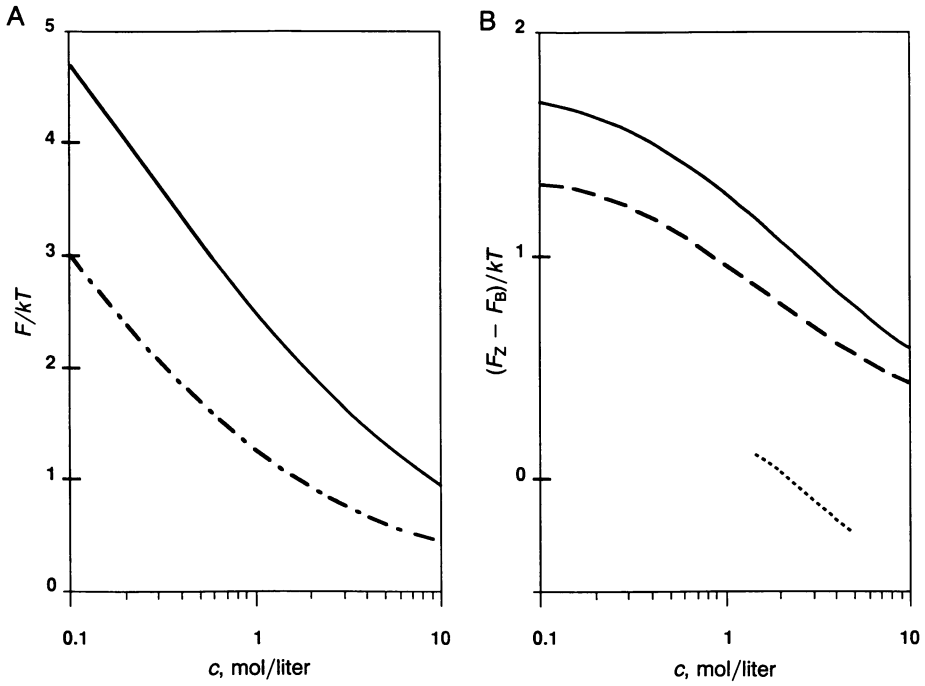

FIG. 2. (*A*) The free energies of B-DNA (solid line) and Z-DNA (dashed and dotted line) as a function of salt concentration in the model of Table 1. Their difference is the solid line in *B*. (*B*) The electrostatic free energy difference per phosphate, versus *c*, the monovalent salt concentration. Solid line, theoretical result for the composite planar model, based on the radii of Table 1. Dashed line, theoretical result for the composite planar model, but with the radii used in ref. 8 (see text). Dotted line, experimental (following ref. 1). Only the slopes should be compared. The solid line agrees well with experiment. The theoretical slope is not greatly affected by the change of the DNA radii.

model, so as to display the quality of the analytical formulae, and also with the results of a numerical Poisson–Boltzmann study of DNA in its exact geometry, so as to evaluate the importance of geometrical details. Such studies require much more computer time than do those described here.

The composite cylinder model could be applied to related problems such as the variation of the relative stability of Z-DNA and B-DNA versus temperature or the A-RNA to Z-RNA transition.

1. Pohl, F. M. (1983) *Cold Spring Harbor Symp. Quant. Biol.* **47**, 113–118.
2. Arnott, S., Campbell-Smith, P. J. & Chandrasekaran, R. (1975) in *CRC Handbook of Biochemistry and Molecular Biology*, ed. Fasman, G. D. (CRC, Cleveland), Vol. 2, pp. 411–423.
3. Guéron, M. & Weisbuch, G. (1980) *Biopolymers* **19**, 353–382.
4. Weisbuch, G. & Guéron, M. (1981) *J. Phys. Chem.* **85**, 517–525.
5. Prock, A. & McConkey, G. (1962) *Topics in Chemical Physics, Based on the Harvard Lectures of Peter J. W. Debye* (Elsevier, Amsterdam), pp. 221–225.
6. Weisbuch, G. & Guéron, M. (1983) *J. Phys. (Paris)* **44**, 251–256.
7. Grahame, D. C. (1947) *Chem. Rev.* **41**, 441–501.
8. Frank-Kamenetskii, M. D., Lukashin, A. V. & Anshelevich, V. V. (1985) *J. Biomol. Struct. Dyn.* **3**, 35–42.
9. Soumpasis, D. M. (1984) *Proc. Natl. Acad. Sci. USA* **81**, 5116–5120.
10. Fixman, M. (1979) *J. Chem. Phys.* **70**, 4995–5005.
11. Wennerstroem, H., Joensson, B. & Linse, P. (1982) *J. Chem. Phys.* **76**, 4665–4670.
12. Anshelevich, V. V., Lukashin, A. V. & Frank-Kamenetskii, M. D. (1984) *Chem. Phys.* **91**, 225–236.
13. Vlachy, V. & Haymet, A. D. J. (1986) *J. Chem. Phys.* **84**, 5874–5880.